



Dang, X., Yang, H., Naafs, B. D. A., Pancost, R. D., & Xie, S. (2016). Evidence of moisture control on the methylation of branched glycerol dialkyl glycerol tetraethers in semi-arid and arid soils. *Geochimica et Cosmochimica Acta*, 189, 24-36. DOI: [10.1016/j.gca.2016.06.004](https://doi.org/10.1016/j.gca.2016.06.004)

Peer reviewed version

Link to published version (if available):
[10.1016/j.gca.2016.06.004](https://doi.org/10.1016/j.gca.2016.06.004)

[Link to publication record in Explore Bristol Research](#)
PDF-document

This is the accepted author manuscript (AAM). The final published version (version of record) is available online via Elsevier at <http://dx.doi.org/10.1016/j.gca.2016.06.004>. Please refer to any applicable terms of use of the publisher.

University of Bristol - Explore Bristol Research

General rights

This document is made available in accordance with publisher policies. Please cite only the published version using the reference above. Full terms of use are available:
<http://www.bristol.ac.uk/pure/about/ebr-terms.html>

1 **Evidence of moisture control on the methylation of branched glycerol dialkyl**
2 **glycerol tetraethers in semi-arid and arid soils**

3
4 Xinyue Dang ^a, Huan Yang ^a, B. David A. Naafs ^b, Richard D. Pancost ^b, Shucheng Xie ^{a,*}

5
6 ^a *State Key Laboratory of Biogeology and Environmental Geology, School of Earth Sciences,*
7 *China University of Geosciences, Wuhan 430074, China*

8 ^b *Organic Geochemistry Unit, Bristol Biogeochemistry Research Centre and The Cabot Institute,*
9 *School of Chemistry, University of Bristol, Cantock's Close, Bristol BS8 1TS, UK*

10
11 *Author to whom correspondence should be addressed (xiecug@163.com)

12
13 **Abstract**

14 The distribution of bacterial branched glycerol dialkyl glycerol tetraethers (brGDGTs) is
15 influenced by growth temperature and pH. This results in the widespread application of the
16 brGDGT-based MBT(′)/CBT proxy (MBT-methylation of branched tetraethers, CBT-cyclization
17 of branched tetraethers) in terrestrial paleo-environmental reconstructions. Recently, it was shown
18 that the amount of precipitation could also have an impact on CBT, as well as the abundance of
19 brGDGTs relative to that of archaeal isoprenoidal (iso)GDGTs ($R_{i/b}$) and the absolute abundance
20 of brGDGTs, potentially complicating the use of MBT/CBT as paleothermometer. However, the
21 full influence of hydrology, and in particular soil water content (SWC), on GDGT distributions
22 remains unclear. Here we investigated variations in the GDGT distribution across a SWC gradient
23 (0-61%) around Qinghai Lake in the Tibetan Plateau, an arid to semiarid region in China. Our
24 results demonstrate that SWC affects the brGDGT distribution. In particular, we show that SWC
25 has a clear impact on the degree of methylation of C6-methylated brGDGTs, whereas
26 C5-methylated brGDGTs are more impacted by temperature. This results in a combined SWC and
27 temperature control on MBT′. In this context we propose a diagnostic parameter, the IR_{6ME}
28 (relative abundance of C6-methylated GDGTs) index, to evaluate the applicability of
29 brGDGT-based paleotemperature reconstructions. Using the global dataset, expanded with our
30 own data, MBT′ has a significant correlation with mean annual air temperature when $IR_{6ME} < 0.5$,

31 allowing for the use of MBT'/CBT as temperature proxy. However, MBT' has a significant
32 correlation with mean annual precipitation (i.e., a substantial reflection of SWC impact) when
33 $IR_{6ME} > 0.5$, implying that MBT' may respond to hydrological change in these regions and can be
34 used as a proxy for MAP.

35

36 **1. Introduction**

37 Lipid biomarkers, including bacterial branched glycerol dialkyl glycerol tetraethers
38 (brGDGTs) and archaeal isoprenoidal (iso)GDGTs, are widely used to reconstruct past
39 environmental conditions in a range of environments (Schouten et al., 2002, 2013; Weijers et al.,
40 2007; Peterse et al., 2012; De Jonge et al., 2014a). Ultimately the reliability of
41 paleo-reconstructions depends on how well the environmental factors controlling these proxies are
42 known in modern settings. Due to the large heterogeneity of terrestrial environments, many
43 proxies, such as the carbon isotopes of organic matter and leaf wax lipids (Zhang et al., 2006;
44 Bendle et al., 2007; Ning et al., 2008; Rao et al., 2013), pollen distributions (Wu et al., 2007) and
45 phytolith distributions (Lu et al., 2006, 2007), appear to be controlled by a range of environmental
46 factors, complicating their interpretation (e.g. ambiguity of temperature vs precipitation control).
47 Consequently, it is necessary to develop new proxies or refine existing ones.

48 BrGDGTs are presumed to be the membrane-spanning lipids of as-yet unknown bacteria
49 that likely favour anaerobic settings (Weijers et al., 2004, 2009, 2010). The occurrence of
50 brGDGTs-Ia (Fig. 1) in some culture isolates of Acidobacteria suggests that these bacteria are
51 likely the producers of at least one of the brGDGTs observed in natural settings (Sinninghe
52 Damsté et al., 2011). The brGDGTs comprise three series (I, II and III) according to their degree
53 of methylation (Weijers et al., 2007), and each series includes components with 0-2 cyclopentyl
54 rings (e.g. Ia, Ib and Ic) (Fig. 1). In global soil datasets, the MBT and modified MBT' proxy,
55 representing two different expressions of the degrees of brGDGT methylation, is empirically
56 related to mean annual air temperature (MAT) and soil pH, whereas the degree of cyclization of
57 brGDGTs, i.e. CBT, correlates only with pH (Weijers et al., 2007; Peterse et al., 2012). A
58 combination of MBT(°) and CBT, i.e., the MBT(°)/CBT proxy, therefore, has been used to
59 reconstruct continental temperature in loess-paleosols (Peterse et al., 2011) and sediments as far
60 back as the Paleocene (Pancost et al., 2013; Kemp et al., 2014). Additional evidence, primarily

61 from altitudinal transects (e. g. [Sinninghe Damsté et al., 2008](#); [Ernst et al., 2013](#)), further supports
62 the close relationship between MBT(°)/CBT and MAT.

63 However, the global soil database is characterized by large scatter in the relationship
64 between MBT' with either MAT or pH ([Peterse et al., 2012](#)), and when applied to modern alkaline
65 soils from semi-arid and arid regions, the global MBT(°)/CBT calibration leads to estimates
66 significantly lower than instrumental temperatures ([Peterse et al., 2012](#); [Yang et al., 2014](#)). These
67 observations imply that other environmental factors impact MBT(°)/CBT and consequently
68 paleo-temperature reconstructions. For example, [Dirghangi et al. \(2013\)](#) suggested that mean
69 annual precipitation (MAP) affects both brGDGT composition and the BIT-index, the ratio of
70 brGDGTs to the dominant isoGDGTs ([Hopmans et al., 2004](#); defined below), in soils from the
71 USA. Similarly, a significant (negative) correlation between CBT and MAP (and SWC) was found
72 in semi-arid and arid soils from China ([Wang et al., 2014](#)). [Menges et al. \(2014\)](#) found that MBT
73 in soils from the Iberian Peninsula had a moderate correlation with the aridity index (AI = mean
74 annual precipitation (MAP)/mean annual potential evapotranspiration), but the effect of MAP on
75 MBT was blurred by its co-variation with pH. MAP has also been proposed to impact the
76 distribution of brGDGTs in cold and wet and in warm and dry regions ([Peterse et al., 2012](#)),
77 although excluding these soils did not improve the relationship with MAT in the global dataset
78 ([Weijers et al., 2007](#); [Peterse et al., 2012](#)), implying that other factors may exist. One such factor
79 could be soil moisture, which at a given site can be decoupled from precipitation. MAP is an
80 annual mean condition of a specific region, but SWC of the same region will also vary with
81 topography, intensity of evapotranspiration, depth of the water table, physical characteristics of
82 soils and soil surface conditions (such as roughness or overlying vegetation) (e.g. [Crave and](#)
83 [Gascuel-Odoux, 1997](#); [Gómez-Plaza et al., 2001](#)). Crucially, it is likely that SWC is a more direct
84 influence on the growth environment of brGDGT-producing bacteria than MAP. Until now,
85 however, the impact of SWC on MBT(°) and GDGT distribution remains unknown, despite the
86 potential implications for MBT(°)/CBT-based paleotemperature reconstructions.

87 More recently, [De Jonge et al. \(2014a\)](#) showed that exclusion of C6-methylated brGDGTs
88 from the MBT(°)/CBT proxy could partly eliminate the deviation of temperature estimates in
89 semi-arid and arid regions. These compounds are the later-eluting isomers of conventional
90 C5-methylated brGDGTs, with at least one methyl at the $\omega/\alpha 6$ position instead of the $\omega/\alpha 5$

91 position in the C5-methylated brGDGTs (De Jonge et al., 2013). Recently, a re-analysis of
92 brGDGTs in global soils by De Jonge et al. (2014a) revealed a close relationship between the
93 abundance of C6-methylated brGDGTs and pH, and the authors inferred different bacterial sources
94 for the two isomers. De Jonge et al. (2014a) also noted that the pH control on the relative
95 abundance of C6-methylated brGDGTs could cause the deviations between MBT'/CBT-derived
96 and actual temperatures in semi-arid and arid regions. The correlation with MAT was improved
97 using the MBT'_{5ME} relationship, in which the C6-methylated brGDGTs are excluded. Nevertheless,
98 the global MBT'_{5ME} calibration overestimated MAT in the cold-dry Qinghai-Tibetan Plateau (Ding
99 et al., 2015), implying other factor(s) controlling MBT'_{5ME} still exist. The higher residual errors of
100 this calibration were usually observed in regions with low MAP (De Jonge et al., 2014a),
101 suggesting the important role of hydrological conditions. However, the proxies based on either
102 C5- or C6-methylated brGDGTs exhibited no relationship with MAP in the global soil dataset (De
103 Jonge et al., 2014a). Consequently, the questions associated with the original MBT/CBT and
104 MBT'/CBT calibrations remain, and it is still unknown whether SWC impacts the distribution of
105 C5- and C6-methylated brGDGTs in soils. Consequently, here we investigate the impacts on
106 brGDGTs composition in a soil transect characterized by changes in SWC but minor variation in
107 temperature and soil pH, to determine the influence of SWC on GDGTs in general and MBT(') in
108 particular.

109

110 **2. Material and methods**

111 *2.1. Sampling*

112 The Qinghai Lake lies in the transitional zone between the Qinghai-Tibetan Plateau (QTP)
113 and Chinese Loess Plateau (CLP) of China (Fig. 2), and is subjected to a typical Asian monsoon
114 climate. Climatic information was obtained from the China Meteorological Data Sharing Service
115 System (<http://cdc.cma.gov.cn/>). The mean annual air and surface soil (upper 5 cm depth)
116 temperature are 0.3 °C and 3.2 °C, respectively. The mean annual precipitation is 373.6 mm,
117 considerably lower than the mean annual evaporation of 1586 mm. A total of 62 soil samples were
118 collected during the wet and dry season (July and March) along several transects perpendicular to
119 the lakeshore to the southeastern of the lake Qinghai (36°33.1'-36°32.8'N, 100°43.6'-100°43.4'E)
120 (Fig. 2), see supplementary information for exact location of samples. Each sample represents a

121 mixture of five subsamples (depth < 3 cm) collected from randomly selected localities in a
122 quadrant (ca. 50cm×50cm). After removal of residual roots, all samples were immediately
123 transported to the laboratory and stored at -20 °C until further analysis.

124

125 *2.2 Environmental variables*

126 SWC was determined for the two contrasting seasons, the rainy/warm season (July) and the
127 cold/dry season (March). Soils are frozen from December to April. The soils were freeze-dried,
128 and the SWC was measured by calculating the difference before and after the freeze drying:

$$129 \text{ SWC} = (W_b - W_a)/W_b \times 100\%$$

130 where W_b and W_a denotes the soil weight before and after the freeze drying. The wet weight was
131 obtained in the field immediately after sampling.

132 Soil pH measurement followed [Weijers et al. \(2007\)](#). Each sample was ground into fine
133 powder using a pestle and mortar and the dry sample was mixed with ultra-pure water in a ratio of
134 1:2.5 (g/ml). The mixture was centrifuged and the pH of the supernatant was measured three times
135 using a pH meter, having a precision of ± 0.01 . The average value of three measurements was
136 taken as the final pH of soil. The soil conductivity was also obtained by measuring the
137 supernatants with a conductivity meter. The soil salinity was determined as the sum of the
138 concentration of major cations (Li^+ , Na^+ , NH_4^+ , K^+ , Mg^{2+} and Ca^{2+}) and anions (F^- , Cl^- , NO_2^- ,
139 SO_4^{2-} , Br^- , NO_3^- and PO_4^{3-}) in the supernatant (soil: water, 1:2.5, g/ml), determined using an ion
140 chromatograph (ICS 600, Thermo Fisher, USA). The in situ temperature for each sampling site
141 was measured in the field using a soil thermometer, although it is important to note that soil
142 temperature is transient and varies within a day.

143

144 *2.3 Lipid extraction*

145 An aliquot of each sample (5-10 g) was extracted with dichloromethane: methanol (9:1, v/v)
146 using an Accelerated Solvent Extractor (ASE 100, Dionex) at temperature of 100 °C and a
147 pressure of 76 bar. The total lipid extract (TLE) was concentrated under reduced pressure by a
148 rotary evaporator. Samples were then base hydrolyzed in 1 M KOH/methanol (5% H_2O in
149 volume) at 80 °C for 2 h. The solution was extracted at least 6 times with *n*-hexane. The combined
150 extracts were dried under a stream of N_2 gas and were then separated into apolar and polar

151 fractions on a silica gel column using *n*-hexane and methanol, respectively. The polar fractions,
152 containing GDGTs, were passed through 0.45 µm PTFE syringe filters and dried under nitrogen
153 gas. We might miss the glycolipids after base hydrolysis, but the GDGTs generated from
154 glycolipids may only represent a minor fraction of total GDGTs and would not influence the
155 distribution and concentration of CL GDGTs.

156

157 2.4. GDGT analysis and proxy calculation

158 The GDGT analyses were performed using Agilent 1200 series liquid
159 chromatography-atmospheric pressure chemical ionization-mass spectrometry (LC-APCI-MS),
160 equipped with autosampler and Masshunter qualitative software. The polar fractions were spiked
161 with an aliquot of internal C₄₆ GDGTs standard (Huguet et al., 2006) and re-dissolved in 300 µl
162 *n*-hexane:ethyl acetate (EtOA) (84:16, v/v). The liquid chromatography methodology followed
163 Yang et al. (2015). The injection volume was 5 µl. Separation of C5- and C6-methylated
164 brGDGTs was achieved using two silica columns in succession (150 mm × 2.1 mm, 1.9 µm,
165 Thermo Finnigan; USA) maintained at 40 °C. GDGTs were first eluted isocratically for the first 5
166 min with 84% A and 16% B, where A = *n*-hexane and B = EtOA. The following elution gradient
167 was used: 84/16 A/B to 82/18 A/B from 5 to 65 min and then to 100% B in 21 min, followed by
168 100% B for 4 min to wash the column and then back to 84/16 A/B to equilibrate it for 30 min at a
169 constant 0.2 ml/min throughout. We scanned for both archaeal isoGDGTs and bacterial brGDGTs
170 using single ion monitoring (SIM) at *m/z* 1302, 1300, 1298, 1296, 1292, 1050, 1048, 1046, 1036,
171 1034, 1032, 1022, 1020, and 1018, to improve the signal to noise ratio. The MS conditions
172 followed Hopmans et al. (2004). GDGTs were quantified from integrated peak areas of the
173 [M+H]⁺ ions. Because we assumed the response factor between the internal standard and
174 respective GDGTs to be 1:1, the concentrations should be considered as semi-quantitative. The
175 C6-methylated brGDGTs were denoted by an accent after the roman numerals for their
176 corresponding C5-methylated isomers.

177 CBT and MBT' were calculated according to the following equations:

$$178 \text{ CBT} = -\log [(Ib+IIb+IIb')/(Ia+IIa+IIa')] \quad (1)$$

$$179 \text{ MBT}' = (Ia+Ib+Ic)/(Ia+Ib+Ic+IIa+IIa'+IIb+IIb'+IIc+IIc'+IIIa+IIIa') \quad (2)$$

180 CBT_{5ME}, MBT'_{5ME}, CBT_{6ME} and MBT'_{6ME} were based on either C5- or C6-methylated

181 brGDGTs (De Jonge et al., 2014a) and calculated as follows:

$$182 \text{ CBT}_{5\text{ME}} = -\log[(\text{Ib}+\text{IIb})/(\text{Ia}+\text{IIa})] \quad (3)$$

$$183 \text{ MBT}'_{5\text{ME}} = (\text{Ia}+\text{Ib}+\text{Ic})/(\text{Ia}+\text{Ib}+\text{Ic}+\text{IIa}+\text{IIb}+\text{IIc}+\text{IIIa}) \quad (4)$$

$$184 \text{ CBT}'_{6\text{ME}} = -\log [(\text{Ib} +\text{IIb}')/(\text{Ia} +\text{IIa}')] \quad (5)$$

$$185 \text{ MBT}'_{6\text{ME}} = (\text{Ia}+\text{Ib}+\text{Ic})/(\text{Ia}+\text{Ib}+\text{Ic} +\text{IIa}' +\text{IIb}' +\text{IIc}' +\text{IIIa}') \quad (6)$$

$$186 \text{ CBT}' = \log[(\text{Ic}+\text{IIa}' +\text{IIb}' +\text{IIc}' +\text{IIIa}' +\text{IIIb}' +\text{IIIc}')/(\text{Ia}+\text{IIa}+\text{IIIa})] \quad (7)$$

187 The BIT index was calculated according to Hopmans et al. (2004):

$$188 \text{ BIT} = (\text{Ia}+\text{IIa}+\text{IIa}' +\text{IIIa}+\text{IIIa}')/(\text{Ia}+\text{IIa}+\text{IIa}' +\text{IIIa}+\text{IIIa}' +\text{crenarchaeol}) \quad (8)$$

189 The $R_{i/b}$ was calculated according to the following equation (Xie et al., 2012):

$$190 R_{i/b} = \sum \text{isoGDGTs} / \sum \text{brGDGTs} \quad (9)$$

191 The fractional abundance of certain brGDGTs was defined as $f(i)$:

$$192 f(5\text{-ME}) = \sum (\text{C5-methylated brGDGTs}) / \sum (\text{all brGDGTs}) \quad (10)$$

$$193 f(6\text{-ME}) = \sum (\text{C6-methylated brGDGTs}) / \sum (\text{all brGDGTs}) \quad (11)$$

$$194 f(\text{I series}) = (\text{Ia}+\text{Ib}+\text{Ic}) / \sum (\text{all brGDGTs}) \quad (12)$$

195 The roman numerals denote the corresponding GDGT structures shown in Fig. 1.

196 The relative amount of C6- vs. C5-methylated brGDGTs was calculated using the following
197 equation (De Jonge et al., 2014b):

$$198 \text{ IR}_{6\text{ME}} = \sum (\text{C6-methylated brGDGTs}) / \sum (\text{C5-methylated brGDGTs} + \text{C6-methylated brGDGTs}) \quad (13)$$

199

200 2.5 Statistical analyses

201 The CANOCO (v. 4.5) software was used to determine the relationship of environmental
202 variables with both the fractional abundances and brGDGTs indices. The environmental variables
203 included SWC, pH, conductivity and salinity of the soil samples. A detrended correspondence
204 analysis (DCA) was performed first and the result showed that the linear model was more
205 appropriate for our dataset because the gradient length was < 2 . The redundancy analysis (RDA)
206 was used to determine the environmental controls on the brGDGT distribution in soils from the
207 SWC transect. The unique contribution of each environmental variable to the variance of GDGT
208 distribution was performed using the partial RDA. The linear regressions between environmental
209 variables and brGDGT-based indices were performed using the SPSS (v. 19.0) software. A p -value
210 < 0.05 indicates a significant correlation.

211

212 **3. Results**

213 *3.1 Environmental variables along the SWC transect*

214 The SWC during our sampling campaign in July ranged from 0 to 61% within the 100-m
215 transect along lake Erhai (Fig. 2). The SWC was lower in March (0 to 30 %), but important in the
216 context of this study is that the SWC gradient was sustained in both seasons.

217 The soil pH varied between 6.8 and 8.6, and showed no relationship with SWC ($R^2 = 0.00$).
218 The *in situ* soil temperature measured during sampling ranged from 14°C to 22°C and showed a
219 weak negative correlation with the SWC ($R^2 = 0.41$, $p < 0.05$); soils with more water could have a
220 higher specific heat capacity than the relatively drier soils. The soil conductivity and salinity had
221 no significant relationship with the SWC ($R^2 = 0.25$ and 0.27 , respectively), indicating that
222 dilution by soil water was not the primary control on the concentration of the ions in these soils.

223

224 *3.2 The concentration and distribution of GDGTs*

225 BrGDGTs and isoGDGTs were detected in all samples. The (semi-quantitative) concentrations
226 of isoGDGTs and brGDGTs ranged from 11 to 82 ng g⁻¹ TOC and from 6.2 to 430 ng g⁻¹ TOC,
227 respectively. The SWC appeared to exert a significant influence on the relative abundance of
228 bacterial brGDGTs and archaeal isoGDGTs (Fig. 3). Bacterial brGDGTs were more abundant than
229 archaeal isoGDGTs in humid soils, but the opposite occurred in soils with SWC < 20% (Fig. 4),
230 corroborating the reliability of $R_{i/b}$ as a drought proxy in Chinese soils (Xie et al., 2012; Yang et al.,
231 2014). The distribution of isoGDGTs was also significantly affected by SWC (Fig. 5a, $0 < p < 0.01$).
232 The acyclic isoGDGT-0 dominated in the relatively high SWC soils, whereas concentrations of
233 isoGDGT-1 to -3 as well as crenarchaeol were higher in soils with low SWC (Fig. 3, 5a). SWC
234 also had a clear impact on the absolute concentration of all brGDGTs, with higher abundance in
235 wetter soils (supplementary Fig. S1). The absolute concentration of bacterial brGDGTs showed no
236 relationship with other environmental variables, including TOC, conductivity, pH and salinity.

237 Crucially, the relative abundance of several brGDGTs was strongly correlated with SWC (Fig.
238 6). BrGDGTs Ia, Ib, and Ic dominated in relatively humid soils, whereas major C6-methylated
239 brGDGT components, including IIIa' and IIa', were most abundant in relatively dry soils (Fig. 6).
240 In particular, the relative abundances of Ib, IIa', IIb' and IIIa' exhibited the highest ($R^2 > 0.69$)

241 correlation with SWC (Fig. 6). The impact of SWC on individual brGDGTs was further supported
242 by the RDA (Fig. 5b). The first two axes explained 74% of the brGDGT variation, with axis 1
243 accounting for 72% of variance; SWC primarily loaded on axis 1 ($p=0.001$), and the partial RDA
244 result showed that SWC alone could explain 39.2% of the variance. SWC appeared to be the
245 dominant control on the brGDGT dataset and the proxies based on them (Fig. 5b, c).
246 C6-methylated brGDGTs and related proxies both exhibited higher correlation coefficients with
247 SWC than C5-methylated isomers (Fig. 5b, c and 6). All the major ions showed no significant
248 relationship with brGDGTs (Fig. 5d), except for Ca^{2+} exhibiting moderate correlations with Iib',
249 IIIa' and Ib.

250

251 **4. Discussion**

252 *4.1 SWC gradient sustained in the transect*

253 In comparison with the rainy season (July), the SWC was lower in the dry winter season
254 (March). However, the SWC gradient was sustained in both seasons (see supplementary
255 information). This is because the gradient is sustained by the lake water via groundwater
256 percolation, not by the precipitation (e.g. Gregorich et al., 2006; Xu et al., 2014). The seasonal
257 variation in absolute SWC will not produce a bias in our investigation of SWC impact on
258 brGDGTs as these depend on the existence of a gradient, not the absolute values of SWC. Indeed,
259 we observe similar relationships for both the wet (below) and dry (supplementary Fig. S2) seasons.
260 However, the choice of season will affect the magnitude of the relationship; because we use July
261 SWC, our correlations reflect a conservative estimate of the SWC-control on GDGTs.

262

263 *4.2 SWC impacts on the degree of methylation of C5- and C6-methylated brGDGTs*

264 Our SWC transect spans only a few hundred meters and as a result is characterized by
265 constant MAT and MAP and a small range of pH, which allows us to assess the influence of soil
266 moisture independent of other variables. The results show that SWC impacts both the
267 concentration and the degree of brGDGT methylation in soils. The ratios of IIIa/IIa and IIIa'/IIa'
268 reflect the degree of methylation of the C5- and C6-methylated brGDGTs, respectively. In our
269 sample set the ratio of IIIa/IIa correlates positively with that of IIIa'/IIa' (Fig. 7a, $R^2 = 0.84$, $p <$
270 0.001), implying that the degree of methylation is controlled by similar factors for both isomers.

271 Moreover, IIIa/IIa and IIIa'/IIa' ratios are both significantly correlated with SWC (Fig. 7b, c; both
272 R^2 are 0.78, $p < 0.001$). This indicates that SWC influences the degree of methylation of both C5-
273 and C6-methylated brGDGTs in our soil samples. However, IIIa'/IIa' ratios exhibit a linear
274 correlation with SWC, whereas the IIIa/IIa ratio appears to have a more complex relationship with
275 SWC, with data falling into two clusters. In relatively humid soils, the %IIIa is considerably lower
276 than %IIa, resulting in a relatively low and constant IIIa/IIa value. In contrast, the %IIIa is higher
277 than %IIa in relatively dry soils, and the ratio of IIIa/IIa has a persistently high value.
278 Consequently, SWC might exert a greater impact on the degree of methylation of C6-methylated
279 brGDGTs compared to that of C5-methylated brGDGTs.

280 The ratios of IIIb/IIb and IIIb'/IIb' (Fig. 7d) are also correlated, albeit with an apparently
281 exponential relationship; the IIIb/IIb and IIIb'/IIb' ratios also exhibit an exponential relationship
282 with the SWC (Fig. 7e, f). Both contrast with the linear relationships seen for IIIa/IIa and IIIa'/IIa'.
283 These results suggest that the response to changes in SWC of brGDGTs containing cyclopentane
284 rings is different compared to those that lack cyclopentane rings.

285 In addition, we find a significant negative correlation between the degree of cyclisation of
286 brGDGTs (CBT) and SWC (Fig. 8a; $R^2 = 0.66$, $p < 0.001$), which is similar to that observed in
287 other studies (Wang et al., 2014). The recently proposed CBT_{6ME} indices, based on C6-methylated
288 brGDGTs (De Jonge et al., 2014a), show higher correlation ($R^2 = 0.7$, $p < 0.001$) with SWC than
289 CBT_{5ME} does ($R^2 = 0.57$, $p < 0.001$) (Fig. 8b, c), further supporting our hypothesis that SWC has a
290 greater impact on C6-methylated brGDGTs than C5-methylated isomers.

291

292 4.3 SWC impacts on MBT'

293 As shown above, both C5- and C6-methylated brGDGTs are impacted by SWC, and our
294 data show a significant positive correlation between MBT' and SWC (Fig. 8d; $R^2 = 0.72$, $p <$
295 0.001), providing an evidence for the impact of soil SWC on the MBT' in soils around Lake Erhai,
296 representative of semi-arid and arid regions of China. The MBT'_{6ME}, based on C6-methylated
297 brGDGTs alone, exhibits a significantly higher correlation with SWC (Fig. 8f; $R^2 = 0.75$, $p <$
298 0.001) than MBT'_{5ME}. This is consistent with our observation that SWC exerts a stronger impact
299 on C6-methylated brGDGTs (further supported by RDA, Fig. 5c). The weaker but significant
300 correlation between MBT'_{5ME} and SWC (Fig. 8e; $R^2 = 0.5$, $p < 0.001$) suggests the possibility that

301 SWC can impact paleotemperature-reconstructions based on MBT'_{5ME}.

302 Nonetheless, it remains unclear how SWC directly or indirectly affects brGDGT
303 distributions. One possibility arises from the impact of SWC on soil specific heat capacity, causing
304 differences in in-situ soil temperature. However, several lines of existing evidence, along with the
305 data in this study, collectively suggest that in-situ soil temperature decreases with increasing SWC
306 (Idso et al., 1975; Wildung et al., 1975; Davidson et al., 1998; Li et al., 2007). This should have
307 resulted in a negative correlation between SWC and MBT', which is opposite to our finding and
308 demonstrates the direct impact of SWC (rather than of temperature) on MBT' in our data set.

309 A recent study on ester-containing phospholipids of bilayers showed that linear-chain
310 phospholipids induced a higher rate of solute and water diffusion compared to branched-chain
311 phospholipids (Balleza et al., 2014). Under drier conditions, the availability of soil water becomes
312 a critical environmental stress for bacterial growth, and we speculate that the brGDGT-producing
313 bacteria could synthesize more branched membrane-lipids to reduce the rate of diffusion, resulting
314 in the observed lower MBT'. Alternatively, SWC could be an indirect control by influencing soil
315 oxygen content. Oxygen content can affect the distribution of bacterial and archaeal communities
316 (Lüdemann et al., 2000; Hansel et al., 2008), and has been argued to control the abundance of
317 brGDGTs in soils as the brGDGTs-producing bacteria are likely to be anaerobic (Weijers et al.,
318 2006a, b). Up to now, previous studies have not suggested that oxygen content could influence
319 brGDGTs distribution, but that possibility cannot be precluded. Oxygen content was not
320 determined in the field, but a first order relationship between SWC and oxygen content in these
321 samples appears to be confirmed by other aspects of the GDGT distribution. The
322 isoGDGT-0/crenarchaeol ratio, which is generally thought to reflect the abundance of anaerobic
323 methanogens (Blaga et al., 2009; Powers et al., 2010), increases significantly with increasing
324 SWC (Fig. 4 and the reference of Wang et al., 2013). The isoGDGT-0/crenarchaeol ratio exhibits
325 weak or moderate correlations with %brGDGTs ($0 < R^2 < 0.52$) and brGDGT-based proxies ($0.4 <$
326 $R^2 < 0.52$), but the relationship between GDGT distributions and oxygen content remains unclear.
327 A third explanation is that changes in the SWC have induced changes in the microbial community,
328 resulting in a change in brGDGT distribution. By extension, it remains unclear whether brGDGTs
329 distributions and brGDGT-based proxies are directly or indirectly controlled by SWC, and future
330 studies should include oxygen content in the suite of characterized environmental parameters.

331 Regardless of mechanism our results do help explain previous observations. For example, In
332 our previous study of soils from Mt. Shennongjia, MBT' had no relationship with temperature, but
333 significant correlation with temperature was observed after eliminating the samples with more
334 C6-methylated brGDGTs than C5-methylated isomers (Yang et al., 2015). This likely reflects the
335 stronger temperature control on C5-methylated brGDGTs (De Jonge et al., 2014a) and the stronger
336 SWC control on C6-methylated brGDGTs. Therefore, temperature controls MBT' in the samples
337 from Mt. Shennongjia when C5-methylated brGDGTs dominate over C6-methylated brGDGTs
338 ($IR_{6ME}=0.10$ to 0.48) (Fig. 9a). Hence, we suggest that the ratio of C6- relative to C5-methylated
339 brGDGTs could be a useful indicator for settings where MBT' is governed primarily by
340 temperature.

341

342 *4.4 Implications for MBT'-based paleoenvironmental reconstruction*

343 As shown above, MBT' could reflect either SWC or temperature, and the relative
344 importance of each can be screened using the relative abundance of C6- or C5-methylated
345 brGDGTs. In order to test this inference, we use the distribution of brGDGTs in the database of
346 global surface soils reported by De Jonge et al. (2014a). Because SWC is not available for the
347 global soil database, we used MAP. MAP is generally correlated with SWC, although SWC is
348 dependent on a wide range of other factors and we recognize that this is only a first order
349 comparison, limited by the global calibration library's metadata.

350 MBT' shows a correlation with both MAT and MAP in the global dataset (Peterse et al.,
351 2012; De Jonge et al., 2014a), with the correlation coefficient being slightly higher with MAP (R^2
352 = 0.58) than with MAT ($R^2 = 0.46$) (De Jonge et al., 2014a), and MAT and MAP explaining
353 relatively equal amounts of the variance (Peterse et al., 2012). It is therefore critical to
354 discriminate the temperature and precipitation controls in paleo-reconstructions. Here we separate
355 the global data set into two groups: arid and humid samples using a rough MAP boundary of
356 500mm. We find that the data show different trends for these two groups (Fig. 10). MBT' exhibits
357 a positive correlation with MAT when $MAP > 500mm$, but not when $MAP < 500mm$, indicating
358 that precipitation (soil moisture content) influences the correlation between MBT' and temperature
359 in the global data set. This will clearly bias paleotemperature reconstructions using the MBT'/CBT
360 proxy in arid regions.

361 The relative abundance of C6- to C5-methylated brGDGTs, as shown above, could provide
362 an independent means to discriminate the relative importance of temperature vs precipitation
363 controls on MBT' in palaeoclimate reconstructions. The global brGDGT dataset (De Jonge et al.,
364 2014a) was separated into two groups, those with IR_{6ME} above and below 0.5 (see supplementary
365 Fig. S4 for the determination of the cut-off value). When IR_{6ME} < 0.5, we found that MBT' shows
366 a significant correlation with MAT (Fig. 11d, R² = 0.71, *p* < 0.05) but a weak correlation with
367 MAP or pH (Fig. 11e, f; R² = 0.36 and 0.19, *p* < 0.05, respectively). This is likely because only a
368 relatively low amount of C6-methylated brGDGTs was present in these soils, and MBT' primarily
369 reflects the variation of MBT'_{5ME}. In contrast, when IR_{6ME} > 0.5, MBT' shows a significant
370 correlation with MAP (Fig. 11h, R² = 0.61, *p* < 0.01) but weak correlation with MAT or pH (Fig.
371 11g, i; R² = 0.35 and 0.27, respectively). This suggests that MBT' can be used as an index for
372 paleoprecipitation reconstructions in regions with IR_{6ME} > 0.5.

373 The relative amount of C6- to C5-methylated brGDGTs is suggested to be primarily
374 controlled by soil pH (De Jonge et al., 2014a; Yang et al., 2015). Similar relationships as those
375 described above, can also be found if the two groups are divided by a soil pH cut-off of 7
376 (supplementary Fig. S5). Nevertheless, the IR_{6ME} is not strictly controlled by pH. In acidic soils,
377 the relative amount of C6-methylated brGDGTs is not always low. Likewise, there are abundant
378 C5-methylated brGDGTs in some alkaline soils. Therefore, application of IR_{6ME} appears to be
379 better than soil pH to discriminate which environmental factor controls the MBT' proxy. In any
380 case, it can be determined directly for palaeoclimate investigations, allowing its direct application
381 in assessing the viability of MBT(')/CBT-based paleotemperature reconstructions.

382

383 5. Conclusions

384 We have investigated the variations in GDGT abundances and distributions in soils along a
385 large SWC gradient in China. SWC has a strong impact on the relative abundance of both
386 brGDGTs and isoGDGTs, as well as the absolute abundance of brGDGTs. Crucially, we show that
387 both the methylation and cyclization of brGDGTs are impacted by SWC. In particular, the degree
388 of methylation of the acyclic C6-methylated brGDGTs exhibits a linear correlation with SWC,
389 whereas that of C5-methylated isomers falls into two clusters. And SWC exerts a greater impact
390 on MBT'_{6ME} compared to MBT'_{5ME}, implying a greater SWC control on the degree of methylation

391 of C6-methylated brGDGTs compared to that of C5-methylated brGDGTs.

392 Our investigation confirms and helps explain previous arguments that paleotemperature
393 reconstruction based on the MBT'/CBT proxy could be biased in arid and semiarid regions.
394 However, our work also reveals that this can be resolved by separating the global dataset into two
395 groups with an IR_{6ME} cut-off of 0.5. We find that MBT' shows a significant correlation with MAT
396 when IR_{6ME} < 0.5 but with MAP (i.e. soil moisture) when IR_{6ME} > 0.5. In alkaline and generally
397 arid regions (like loess-palaeosol sequences), the soil water availability seems to be more
398 important under a condition of water scarcity and the relative amount of C6-methylated brGDGTs
399 is generally high, thus the influence of SWC on MBT' will be obvious and result in a large
400 deviation of reconstructed temperature in these regions. Therefore, the IR_{6ME} can be used to assess
401 whether application of the MBT'(/CBT proxy is appropriate in paleotemperature reconstructions.

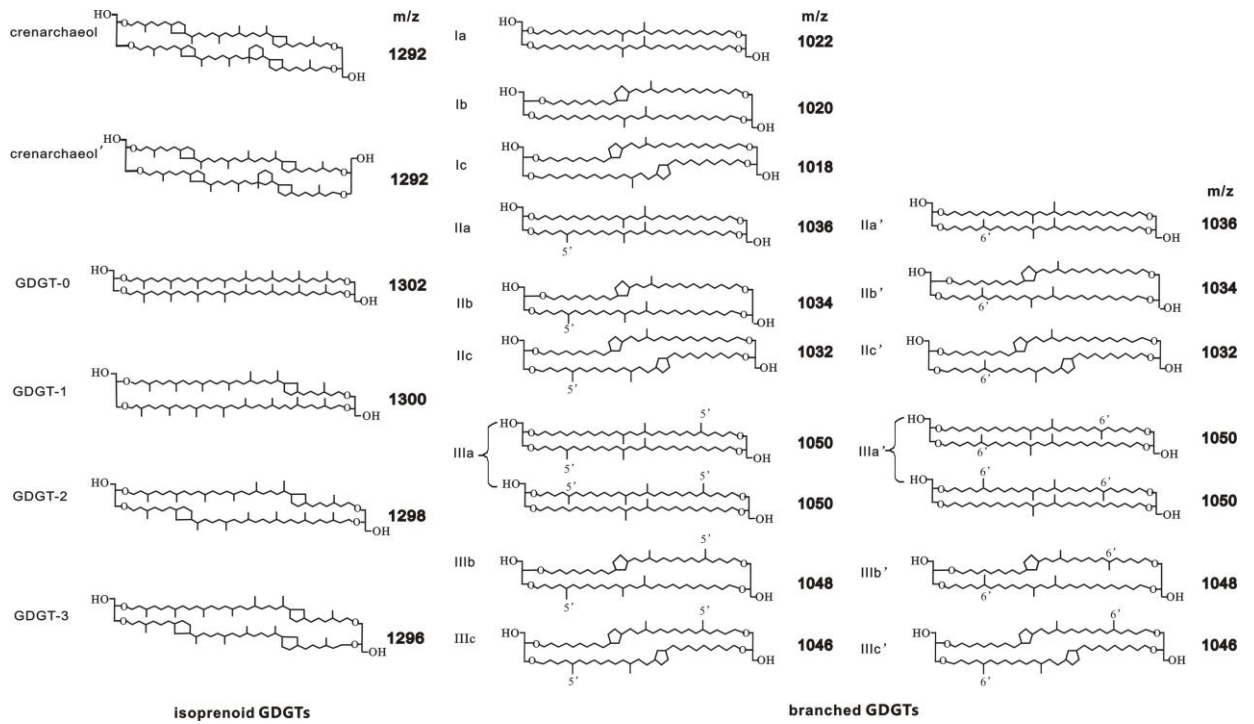
402

403 **Acknowledgements**

404 We thank Alex Sessions and three anonymous reviewers who provided valuable comments on the
405 manuscript, and thank Zhixin Han, Jiangsi Liu, Bingyan Zhao, Wenjie Xiao, Jiayi Lu and Ruicheng
406 Wang for soil sampling. This work was supported by Natural Science Foundation of China (Grant
407 No. 41330103) and 111 Project (Grant No. B08030) and the Special Fund for Basic Scientific
408 Research of Central Colleges, China University of Geosciences, Wuhan (Grant No.
409 CUGL150812).

410

411 **Figures and figure captions**

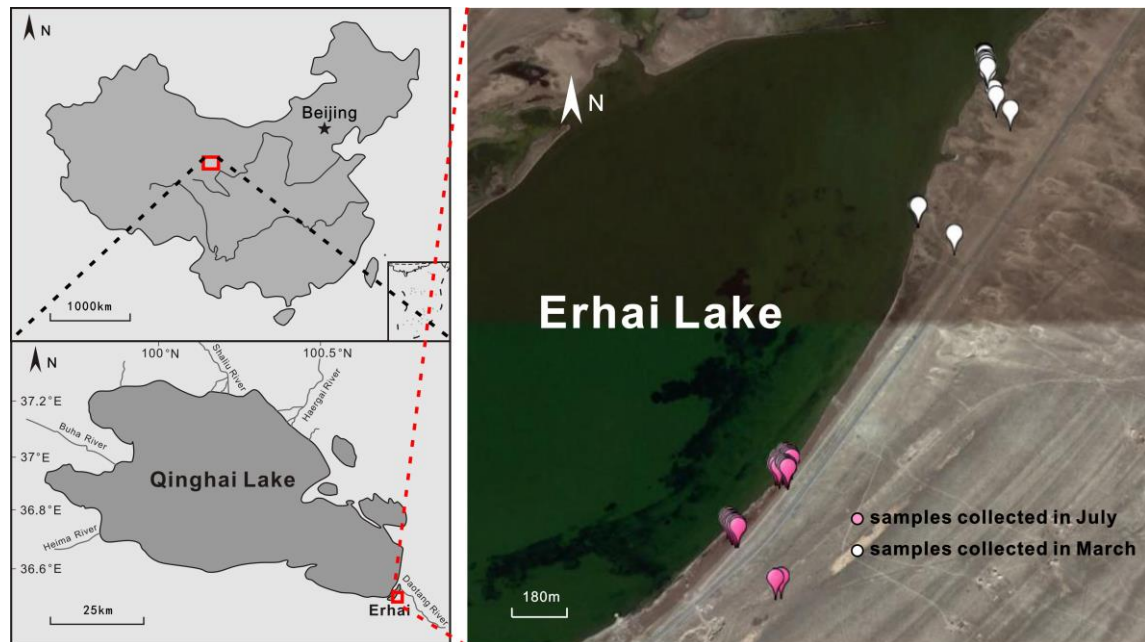


412

413 Fig. 1 The structures of archaeal isoprenoidal (iso-) and bacterial branched (br-) glycerol dialkyl

414 glycerol tetraethers (GDGTs)

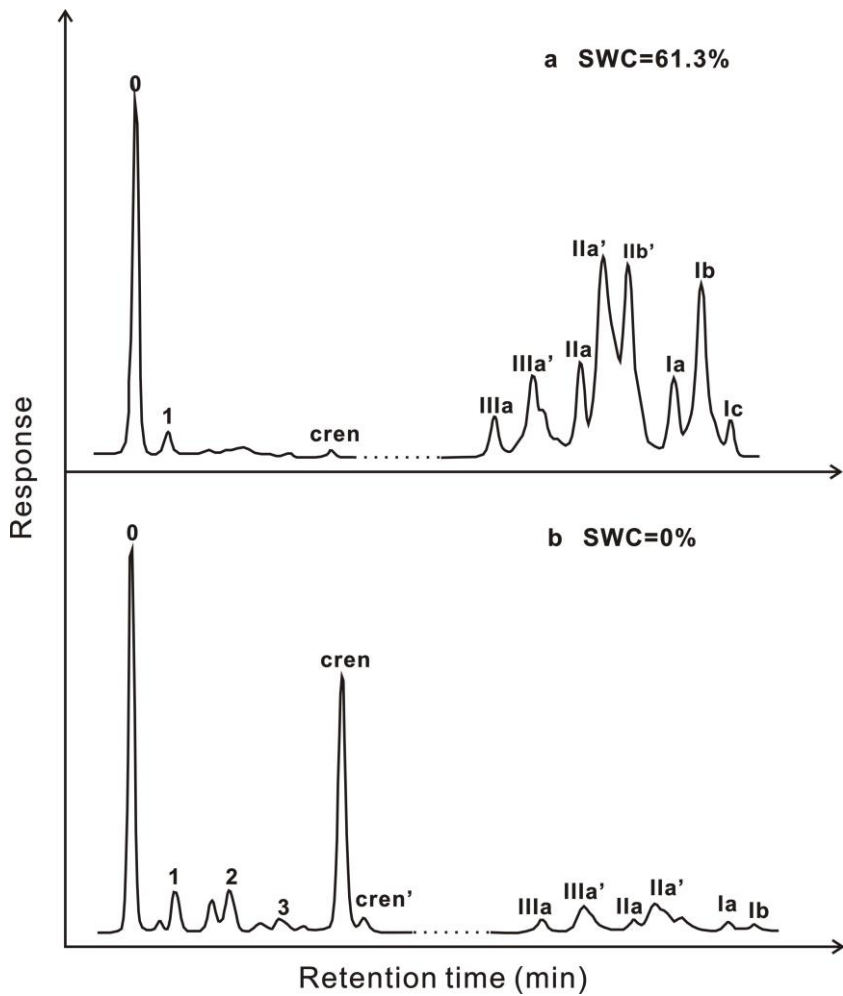
415



416

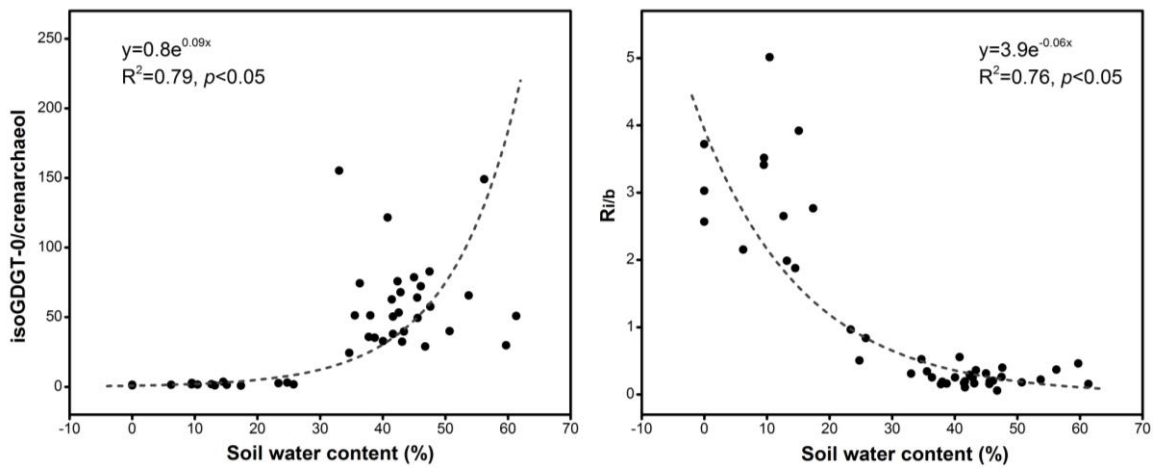
417 Fig. 2 Sketch map of sampling site (n = 62)

418



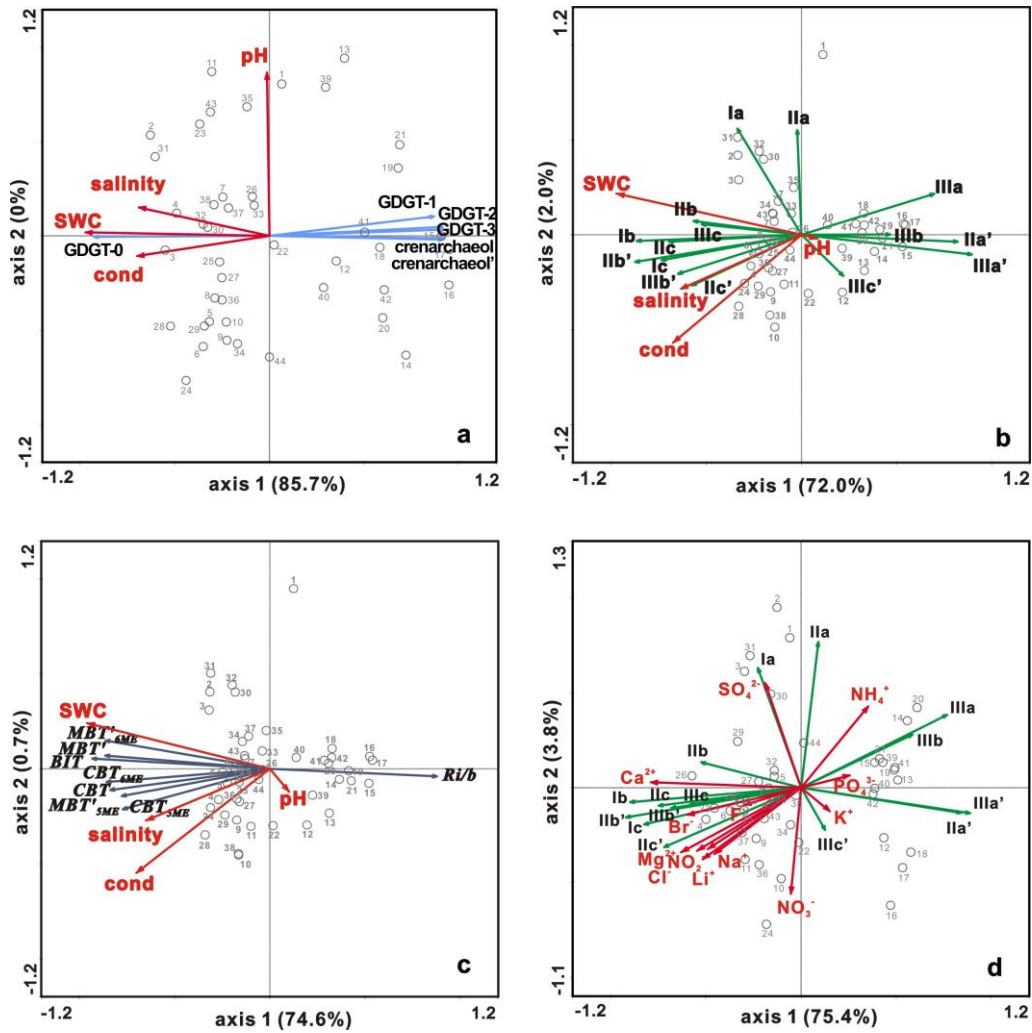
419
420
421

Fig. 3 Partial base peak chromatograms of GDGTs in selected soil samples with different SWC



422
423
424

Fig. 4 Scatter plots of SWC against isoGDGT-0/crenarchaeol (left) and Ri/b (right).



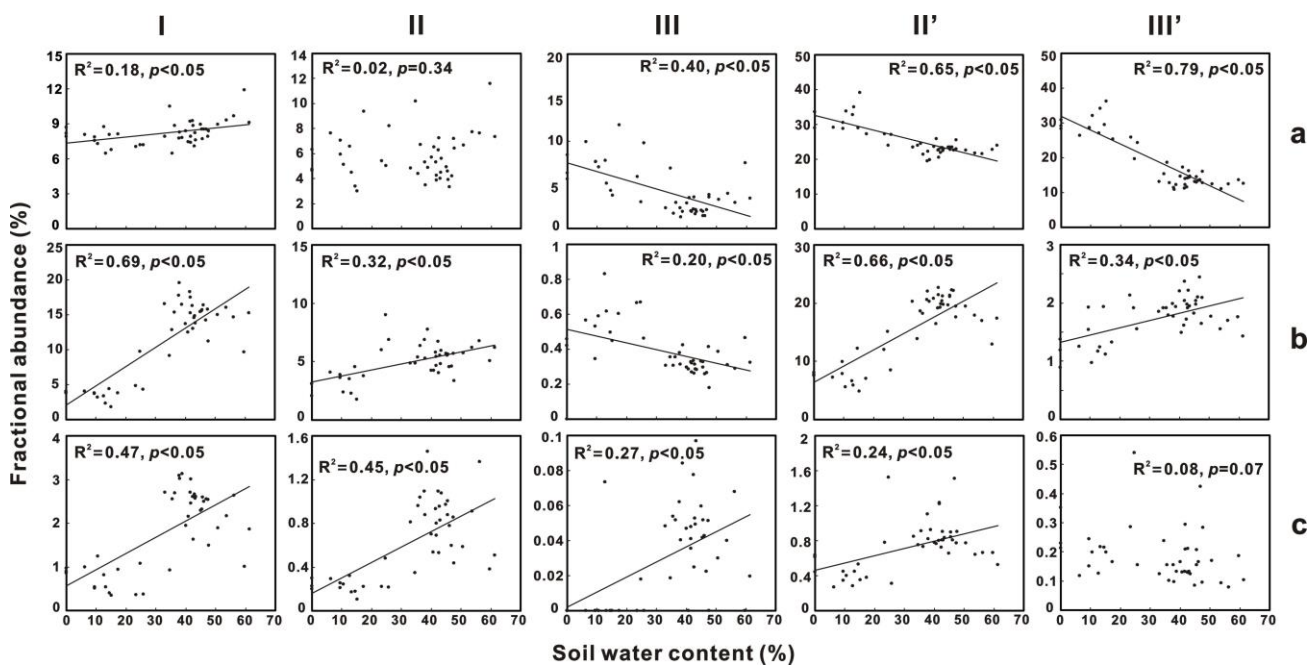
425

426 Fig. 5 RDA triplots showing the relationships of environmental variables with (a) isoGDGTs, (b)

427 brGDGTs, and (c) related proxies; and (d) the relationship of major ions with brGDGTs. 'Cond'

428 means conductivity.

429

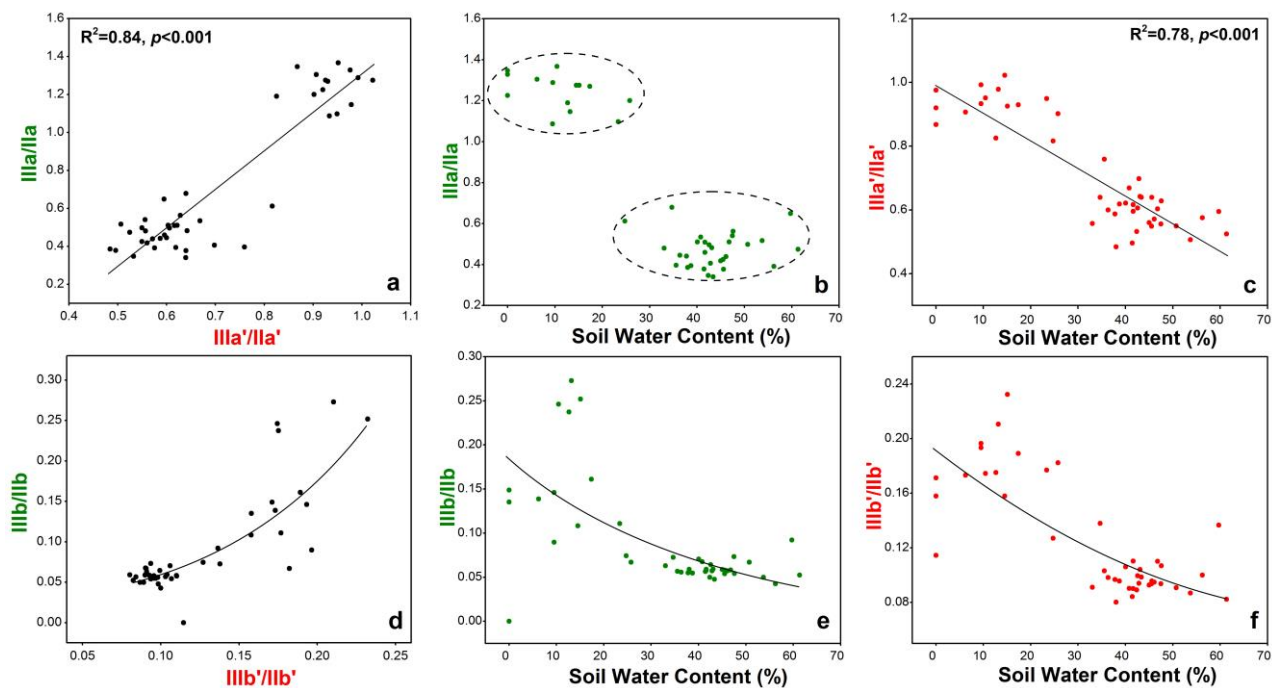


430

431 Fig. 6 Fractional abundance of brGDGTs plotted vs. soil water content. The roman numbers refer

432 to the structures in Fig. 1.

433

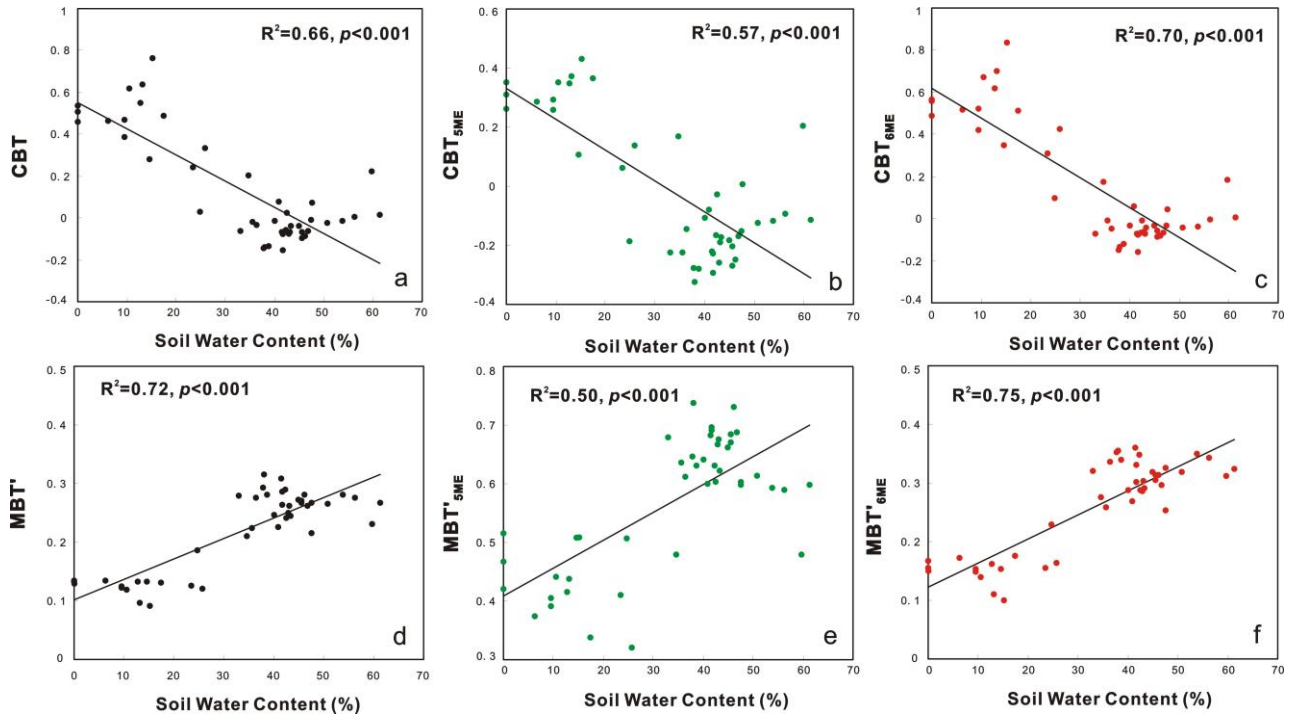


434

435 Fig. 7 Scatter plot between brGDGT ratios and between one of the ratios with SWC, showing the

436 variation of methylation degree of C5- and C6-methylated brGDGTs with SWC.

437

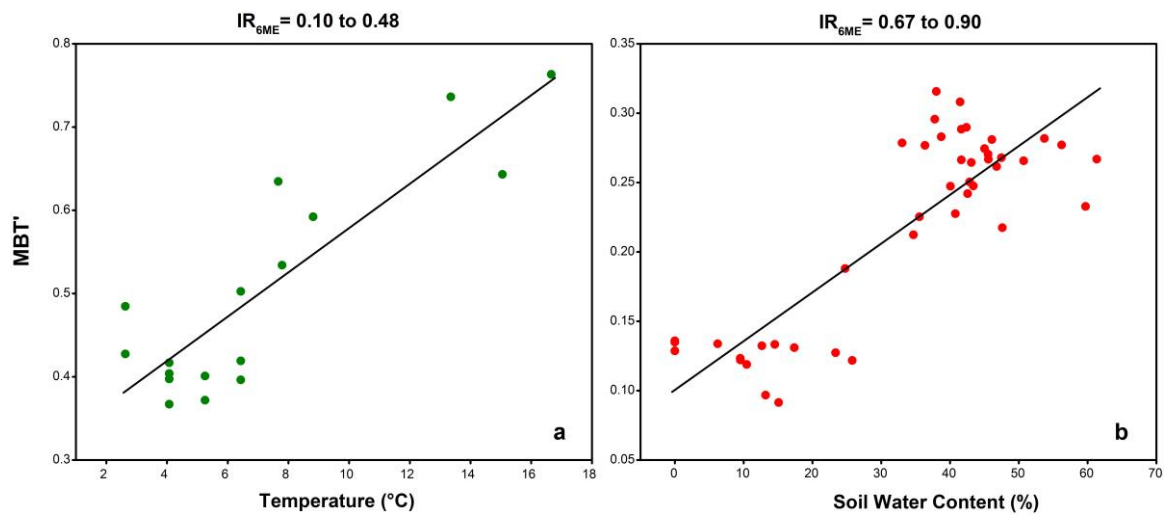


438

439 Fig. 8 Scatter plots of soil water content with brGDGT parameters: (a) CBT; (b) CBT_{5ME}; (c)

440 CBT_{6ME}; (d) MBT'; (e) MBT'_{5ME}; (f) MBT'_{6ME}.

441



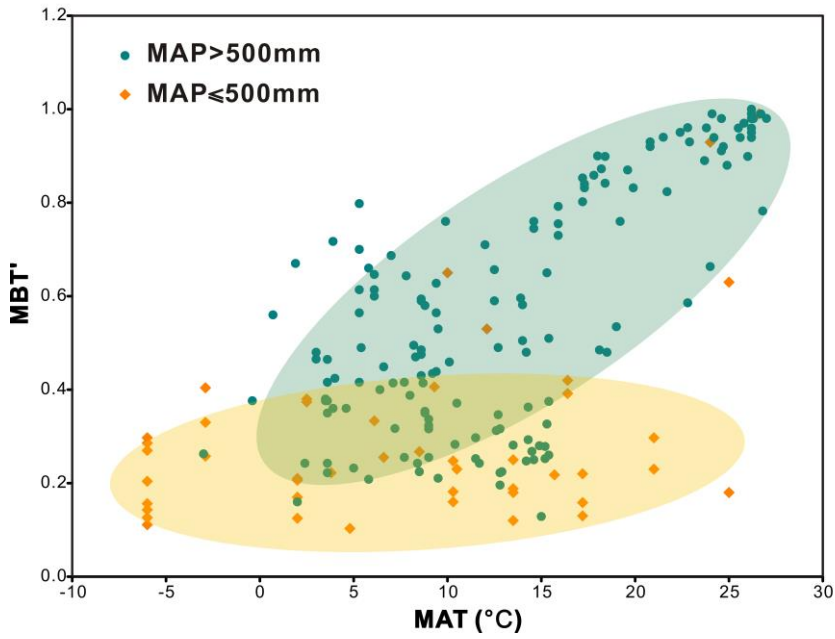
442

443 Fig. 9 Scatter plots of MBT' with air temperature in soils from Mt. Shennongjia with more

444 C5-methylated brGDGTs than C6-methylated isomers (Yang et al., 2015) (a) or with SWC in

445 Qinghai lake region of this study with higher abundance of C6-methylated brGDGTs (b).

446

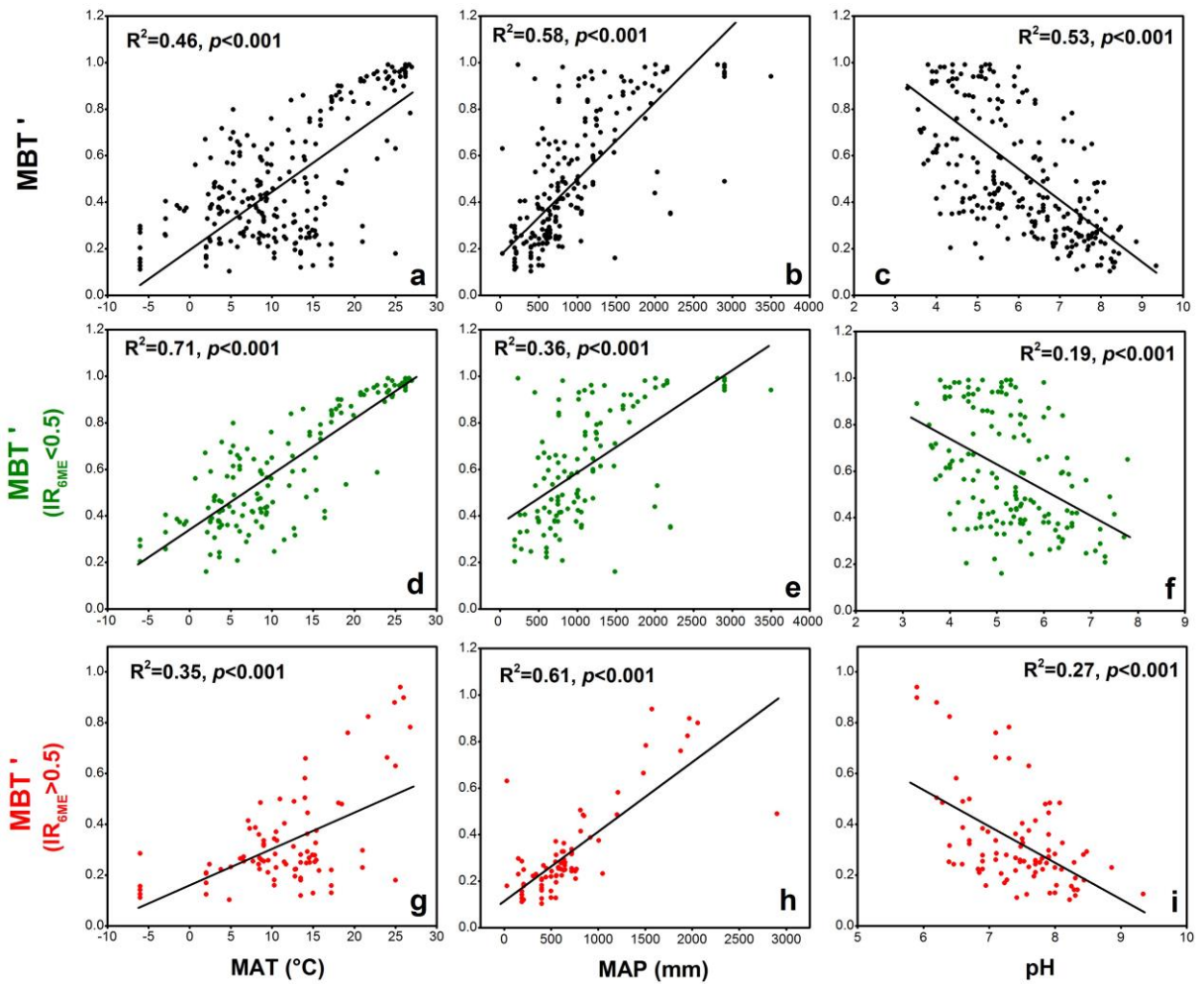


447

448 Fig. 10 Scatter plot of MBT' vs. MAT for the global dataset (De Jonge et al., 2014a) separated

449 into two groups according to MAP.

450



451

452 Fig. 11 Plots of MBT' with MAT (a, d, g), MAP (b, e, h) or pH (c, f, i) for the global dataset (De
453 Jonge et al., 2014a) . The black dots (a, b, c) are all the global data (De Jonge et al., 2014a), the
454 green dots (d, e, f) are soil samples with more C5-methylated brGDGTs ($IR_{6ME}<0.5$), and the red
455 dots (g, h, i) are soils containing more C6-methylated brGDGTs ($IR_{6ME}>0.5$).

456

457

458 **References**

459 Balleza, D., Garcia-Arribas, Aritz B., Sot, J., Ruiz-Mirazo, K., Goñi, Félix M., (2014) Ether- versus
460 ester-linked phospholipid bilayers containing either linear or branched apolar chains. *Biophysical*
461 *Journal*. **107**, 1364-1374.

462 Bendle, J., Kawamura, K., Yamazaki, K., Niwai, T., (2007) Latitudinal distribution of terrestrial lipid
463 biomarkers and n-alkane compound-specific stable carbon isotope ratios in the atmosphere over the
464 western Pacific and Southern Ocean. *Geochimica et Cosmochimica Acta*. **71**, 5934-5955.

465 Blaga, C.I., Reichart, G.-J., Heiri, O., Sinninghe Damsté, J.S., (2009) Tetraether membrane lipid
466 distributions in water-column particulate matter and sediments: a study of 47 European lakes along
467 a north–south transect. *Journal of Paleolimnology*. **41**, 523-540.

468 Crave, A., Gascuel-Oudou, C., (1997) The influence of topography on time and space distribution
469 of soil surface water content. *Hydrological Processes*. **11**, 203-210.

470 Davidson, E., Belk, E., Boone, R.D., (1998) Soil water content and temperature as independent or
471 confounded factors controlling soil respiration in a temperate mixed hardwood forest. *Global*
472 *Change Biology*. **4**, 217-227.

473 De Jonge, C., Hopmans, E.C., Stadnitskaia, A., Rijpstra, W.I.C., Hofland, R., Tegelaar, E., Sinninghe
474 Damsté, J.S., (2013) Identification of novel penta- and hexamethylated branched glycerol dialkyl
475 glycerol tetraethers in peat using HPLC–MS2, GC–MS and GC–SMB-MS. *Organic Geochemistry*.
476 **54**, 78-82.

477 De Jonge, C., Hopmans, E.C., Zell, C.I., Kim, J.-H., Schouten, S., Sinninghe Damsté, J.S., (2014a)
478 Occurrence and abundance of 6-methyl branched glycerol dialkyl glycerol tetraethers in soils:
479 Implications for palaeoclimate reconstruction. *Geochimica et Cosmochimica Acta*. **141**, 97-112.

480 De Jonge, C., Stadnitskaia, A., Hopmans, E.C., Cherkashov, G., Fedotov, A., Sinninghe Damsté, J.S.,
481 (2014b) In situ produced branched glycerol dialkyl glycerol tetraethers in suspended particulate

482 matter from the Yenisei River, Eastern Siberia. *Geochimica et Cosmochimica Acta*. **125**, 476-491.

483 Ding, S., Xu, Y., Wang, Y., He, Y., Hou, J., Chen, L., He, J.S., (2015) Distribution of branched glycerol
484 dialkyl glycerol tetraethers in surface soils of the Qinghai–Tibetan Plateau: implications of
485 brGDGTs-based proxies in cold and dry regions. *Biogeosciences*. **12**, 3141-3151.

486 Dirghangi, S.S., Pagani, M., Hren, M.T., Tipple, B.J., (2013) Distribution of glycerol dialkyl glycerol
487 tetraethers in soils from two environmental transects in the USA. *Organic Geochemistry*. **59**, 49-60.

488 Ernst, N., Peterse, F., Breitenbach, S.F.M., Syiemlieh, H.J., Eglinton, T.I., (2013) Biomarkers record
489 environmental changes along an altitudinal transect in the wettest place on Earth. *Organic*
490 *Geochemistry*. **60**, 93-99.

491 Gómez-Plaza, A., Martínez-Mena, M., Albaladejo, J., Castillo, V.M., (2001) Factors regulating
492 spatial distribution of soil water content in small semiarid catchments. *Journal of Hydrology*.
493 **253**, 211-226.

494 Gregorich, E.G., Hopkins, D.W., Elberling, E., Sparrow, A.D., Novis, P., Greenfield, L.G.,
495 Rochette, P., (2006) Emission of CO₂, CH₄ and N₂O from lakeshore soils in an Antarctic dry
496 valley. *Soil Biology and Biochemistry*. **38**, 3120-3129.

497 Hansel, C.M., Fendorf, S., Jardine, P.M., Francis, C.A., (2008) Changes in Bacterial and Archaeal
498 Community Structure and Functional Diversity along a Geochemically Variable Soil Profile.
499 *Applied and Environmental Microbiology*. **74**, 1620-1633.

500 Hopmans, E.C., Weijers, J.W., Schefuß, E., Herfort, L., Sinninghe Damsté, J.S., Schouten, S., (2004) A
501 novel proxy for terrestrial organic matter in sediments based on branched and isoprenoid tetraether
502 lipids. *Earth and Planetary Science Letters*. **224**, 107-116.

503 Huguet, C., Hopmans, E.C., Febo-Ayala, W., Thompson, D.H., Sinninghe Damsté, J.S., Schouten, S.,
504 (2006) An improved method to determine the absolute abundance of glycerol dibiphytanyl glycerol
505 tetraether lipids. *Organic Geochemistry*. **37**, 1036-1041.

506 Idso, S., Schmugge, T., Jackson, R., Reginato, R., (1975) The utility of surface temperature
507 measurements for the remote sensing of surface soil water status. *Journal of Geophysical Research*.
508 **80**, 3044-3049.

509 Kemp, D.B., Robinson, S.A., Crame, J.A., Francis, J.E., Ineson, J., Whittle, R.J., Bowman, V., O'Brien,
510 C., (2014) A cool temperate climate on the Antarctic Peninsula through the latest Cretaceous to
511 early Paleogene. *Geology*. **42**, 583-586.

512 Li, H.X., Xia, Z.Q., Ma, G. H., (2007) Effects of water content variation on soil temperature process
513 and water exchange [J]. *Journal of Hohai University (Natural Sciences)*. **2**, 011.

514 Lu, H.Y., Wu, N.Q., Yang, X.D., Jiang, H., Liu, K.B., Liu, T.S., (2006) Phytoliths as quantitative
515 indicators for the reconstruction of past environmental conditions in China I: phytolith-based
516 transfer functions. *Quaternary Science Reviews*. **25**, 945-959.

517 Lu, H.Y., Wu, N.Q., Liu, K.B., Jiang, H., Liu, T.S., (2007) Phytoliths as quantitative indicators for the
518 reconstruction of past environmental conditions in China II: palaeoenvironmental reconstruction in
519 the Loess Plateau. *Quaternary Science Reviews*. **26**, 759-772.

520 Lüdemann, H., Arth, I., Liesack, W., (2000) Spatial Changes in the Bacterial Community Structure
521 along a Vertical Oxygen Gradient in Flooded Paddy Soil Cores. *Applied and Environmental*
522 *Microbiology*. **66**, 754-762.

523 Menges, J., Huguet, C., Alcañiz, J., Fietz, S., Sachse, D., Rosell-Melé, A., (2014) Influence of water
524 availability in the distributions of branched glycerol dialkyl glycerol tetraether in soils of the
525 Iberian Peninsula. *Biogeosciences*. **11**, 2571-2581.

526 Ning, Y., Liu, W., An, Z., (2008) A 130-ka reconstruction of precipitation on the Chinese Loess Plateau
527 from organic carbon isotopes. *Palaeogeography, Palaeoclimatology, Palaeoecology*. **270**, 59-63.

528 Pancost, R.D., Taylor, K.W.R., Inglis, G.N., Kennedy, E.M., Handley, L., Hollis, C.J., Crouch, E.M.,
529 Pross, J., Huber, M., Schouten, S., Pearson, P.N., Morgans, H.E.G., Raine, J.I., (2013) Early
530 Paleogene evolution of terrestrial climate in the SW Pacific, Southern New Zealand. *Geochemistry,*
531 *Geophysics, Geosystems*. **14**, 5413-5429.

532 Peterse, F., Prins, M.A., Beets, C.J., Troelstra, S.R., Zheng, H., Gu, Z., Schouten, S., Damsté, J.S.S.,
533 (2011) Decoupled warming and monsoon precipitation in East Asia over the last deglaciation. *Earth*
534 *and Planetary Science Letters*. **301**, 256-264.

535 Peterse, F., van der Meer, J., Schouten, S., Weijers, J.W., Fierer, N., Jackson, R.B., Kim, J.-H.,
536 Sinninghe Damsté, J.S., (2012) Revised calibration of the MBT–CBT paleotemperature proxy
537 based on branched tetraether membrane lipids in surface soils. *Geochimica et Cosmochimica Acta*.
538 **96**, 215-229.

539 Powers, L., Werne, J.P., Vanderwoude, A.J., Sinninghe Damsté, J.S., Hopmans, E.C., Schouten, S.,
540 (2010) Applicability and calibration of the TEX86 paleothermometer in lakes. *Organic*
541 *Geochemistry*. **41**, 404-413.

542 Rao, Z., Chen, F., Cheng, H., Liu, W., Wang, G.a., Lai, Z., Bloemendal, J., (2013) High-resolution
543 summer precipitation variations in the western Chinese Loess Plateau during the last glacial. *Sci.*
544 *Rep.* **3**.

545 Schouten, S., Hopmans, E.C., Schefuß, E., Sinninghe Damsté, J.S., (2002) Distributional variations in
546 marine crenarchaeotal membrane lipids: a new tool for reconstructing ancient sea water
547 temperatures? *Earth and Planetary Science Letters.* **204**, 265-274.

548 Schouten, S., Hopmans, E.C., Sinninghe Damsté, J.S., (2013) The organic geochemistry of glycerol
549 dialkyl glycerol tetraether lipids: A review. *Organic Geochemistry.* **54**, 19-61.

550 Sinninghe Damsté, J.S., Ossebaar, J., Schouten, S., Verschuren, D., (2008) Altitudinal shifts in the
551 branched tetraether lipid distribution in soil from Mt. Kilimanjaro (Tanzania): Implications for the
552 MBT/CBT continental palaeothermometer. *Organic Geochemistry.* **39**, 1072-1076.

553 Sinninghe Damsté, J.S., Rijpstra, W.I.C., Hopmans, E.C., Weijers, J.W.H., Foesel, B.U., Overmann, J.,
554 Dedysh, S.N., (2011) 13,16-Dimethyl Octacosanedioic Acid (iso-Diabolic Acid), a Common
555 Membrane-Spanning Lipid of Acidobacteria Subdivisions 1 and 3. *Applied and Environmental*
556 *Microbiology.* **77**, 4147-4154.

557 Wang, H., Liu, W., Zhang, C.L., Liu, Z., He, Y., (2013) Branched and isoprenoid tetraether (BIT) index
558 traces water content along two marsh-soil transects surrounding Lake Qinghai: Implications for
559 paleo-humidity variation. *Organic Geochemistry.* **59**, 75-81.

560 Wang, H., Liu, W., Zhang, C., (2014) Dependence of the cyclization of branched tetraethers on soil
561 moisture in alkaline soils from arid–subhumid China: implications for palaeorainfall
562 reconstructions on the Chinese Loess Plateau. *Biogeosciences.* **11**, 6755-6768.

563 Weijers, J.W.H., Schouten, S., van der Linden, M., van Geel, B., Sinninghe Damsté, J.S., (2004) Water
564 table related variations in the abundance of intact archaeal membrane lipids in a Swedish peat bog.
565 *Fems Microbiology Letters.* **239**, 51-56.

566 Weijers, J.W.H., Schouten, S., Hopmans, E.C., Geenevasen, J.A.J., David, O.R.P., Coleman, J.M.,
567 Pancost, R.D., Sinninghe Damsté, J.S., (2006a) Membrane lipids of mesophilic anaerobic bacteria
568 thriving in peats have typical archaeal traits. *Environmental Microbiology.* **8**, 648-657.

569 Weijers, J.W.H., Schouten, S., Spaargaren, O.C., Sinninghe Damsté, J.S., (2006b) Occurrence and
570 distribution of tetraether membrane lipids in soils: Implications for the use of the TEX86 proxy and
571 the BIT index. *Organic Geochemistry.* **37**, 1680-1693.

572 Weijers, J.W.H., Schouten, S., van den Donker, J.C., Hopmans, E.C., Sinninghe Damsté, J.S., (2007)
573 Environmental controls on bacterial tetraether membrane lipid distribution in soils. *Geochimica et*
574 *Cosmochimica Acta.* **71**, 703-713.

575 Weijers, J.W.H., Panoto, E., van Bleijswijk, J., Schouten, S., Rijpstra, W.I.C., Balk, M., Stams, A.J.,
576 Sinninghe Damsté, J.S., (2009) Constraints on the biological source (s) of the orphan branched
577 tetraether membrane lipids. *Geomicrobiology Journal.* **26**, 402-414.

578 Weijers, J.W.H., Wiesenberg, G., Bol, R., Hopmans, E., Pancost, R., (2010) Carbon isotopic
579 composition of branched tetraether membrane lipids in soils suggest a rapid turnover and a
580 heterotrophic life style of their source organism (s). *Biogeosciences Discussions.* **7**, 3691-3734.

581 Wildung, R., Garland, T., Buschbom, R., (1975) The interdependent effects of soil temperature and
582 water content on soil respiration rate and plant root decomposition in arid grassland soils. *Soil*
583 *Biology and Biochemistry.* **7**, 373-378.

584 Wu, F., Fang, X., Ma, Y., Herrmann, M., Mosbrugger, V., An, Z., Miao, Y., (2007) Plio–Quaternary
585 stepwise drying of Asia: Evidence from a 3-Ma pollen record from the Chinese Loess Plateau.
586 *Earth and Planetary Science Letters.* **257**, 160-169.

587 Xie, S., Pancost, R.D., Chen, L., Evershed, R.P., Yang, H., Zhang, K., Huang, J., Xu, Y., (2012)
588 Microbial lipid records of highly alkaline deposits and enhanced aridity associated with significant
589 uplift of the Tibetan Plateau in the Late Miocene. *Geology.* **40**, 291-294.

590 Xu, X., Zhang, Q., Li, Y., Li, X., Wang, X., (2014) Inner-annual variation of soil water content and
591 groundwater level in a typical islet wetland of Lake Poyang. *Journal of Lake Sciences.* **26**, 260-268.

592 Yang, H., Pancost, R.D., Dang, X., Zhou, X., Evershed, R.P., Xiao, G., Tang, C., Gao, L., Guo, Z., Xie,
593 S., (2014) Correlations between microbial tetraether lipids and environmental variables in Chinese
594 soils: Optimizing the paleo-reconstructions in semi-arid and arid regions. *Geochimica et*
595 *Cosmochimica Acta.* **126**, 49-69.

596 Yang, H., Lü, X., Ding, W., Lei, Y., Dang, X., Xie, S., (2015) The 6-methyl branched tetraethers
597 significantly affect the performance of the methylation index (MBT') in soils from an altitudinal
598 transect at Mount Shennongjia. *Organic Geochemistry.* **82**, 42-53.

599 Zhang, Z., Zhao, M., Eglinton, G., Lu, H., Huang, C. Y., (2006) Leaf wax lipids as paleovegetational
600 and paleoenvironmental proxies for the Chinese Loess Plateau over the last 170 kyr. *Quaternary*
601 *Science Reviews.* **25**, 575-594.